Supplementary Information

Analysis of Flood Drivers Contributions to Compound Flooding Using Coupled Modeling and Machine Learning

Javed Ali[1], Sadaf Mahmoudi[2], Farnaz Yarveysi[3], Samuel Daramola[4]

[1]University of Central Florida; *javed.ali@ucf.edu*

[2]University of Alabama, Tuscaloosa; *smahmoudikouhi@crimson.ua.edu*

[3]University of Alabama, Tuscaloosa; *fyarveysi@crimson.ua.edu*

[4]Virginia Tech, Blacksburg; *samueldaramola@vt.edu*

Academic Advisors: Thomas Wahl, *University of Central Florida*[1]; Hamed Moftakhari, *University of Alabama*[2]; Hamid Moradkhani, *University of Alabama*[3]; David Muñoz, *Virginia Tech*[4]

Summer Institute Theme Advisor: Kyle T. Mandli, Columbia University, *kyle.mandli@columbia.edu*

Methodology

1. Hydrologic Modeling using NWC CFE Model

The National Water Center's Conceptual Functional Equivalent (CFE) model is a conceptual rainfall-runoff model, which is designed to simulate how rainfall gets converted into runoff, a key process in understanding how much water will flow into rivers and streams after a rain event.

1.2 Generation of HydroFabric Subsets

The first stage of hydrologic modeling with CFE involves the acquisition and processing of HydroFabric data specific to the eight delineated watersheds within the study area. The hydrological data were retrieved from the Amazon S3 Bucket (https://nextgen-hydrofabric.s3.amazonaws.com). Subsequent to retrieval, the necessary information was extracted and processed for the construction of parameter configuration files.

1.3 Parameter Configuration for Hydrological Modeling

The parameter configuration files play an important role in facilitating the operation of the Conceptual Functional Equivalent (CFE) model and the Simple Logical Tautology Handler (SLoTH) within the context of the NextGen framework. These files comprise a variety of components, including model default parameters, specific formulations, detailed input and output paths, simulation time steps, and initial conditions. Furthermore, they encapsulate additional settings that are pertinent to the accurate modeling of the hydrological system under study.

1.4 Preparation of Basin-Averaged Forcing Inputs

The next step in this process is the generation of basin-averaged forcing inputs, each tailored to match distinct storm event time periods within the eight individual watersheds of the study area. The input data, extracted from AORC v1.0 kerchunk header files, is prepared specifically for integration with NOAA's advanced Next Generation (NextGen) Water Resource Modeling Framework.

1.5 Execution of the CFE Model within the NGEN Framework

For running the CFE model within the NGEN framework using BMI, we used the ngen command that combines the positional arguments for the execution of the CFE model. For details, see the GitHub repository.

Results

1. Hydrodynamic Model Validation:

Figure S1 shows the comparison between the simulation and observation time series at the time of the storm's peak during Hurricane Sandy. Unlike Hurricane Irene, the model encounters challenges in accurately representing the water levels prior to being influenced by storm events during Hurricane Sandy. Specifically, during Hurricane Sandy, GeoClaw exhibited the ability to capture the fluctuations in water levels but failed to accurately reproduce the maximum values. Consequently, despite the implementation of the maximum bias correction technique, the figures obtained after bias correction only succeeded in capturing the maximum values, rather than accurately representing the values preceding the storm. These observations suggest limitations in GeoClaw's ability to adequately simulate the pre-storm water levels and the associated dynamics. It is important to acknowledge these limitations when interpreting the model's results and assessing its overall performance. Future research endeavors may focus on refining the model's capabilities in capturing pre-storm water levels by exploring alternative model configurations, incorporating additional data sources, or refining parameterizations to improve the simulation of coastal processes.

Moreover, evaluation metrics of the biased corrected and not biased corrected simulation results of Hurricane Sandy are shown in Table S1. The Montauk Station experienced a deterioration in evaluation metrics following bias correction during Hurricane Irene, while the Kings Point Station exhibited worsened evaluation metrics after bias correction during Hurricane Sandy. In contrast, the remaining monitoring stations demonstrated improved evaluation metrics following the application of bias correction. The observed enhancements in evaluation metrics at most of the monitoring stations suggest the effectiveness of bias correction in improving the agreement between modeled and observed data. The positive impact of bias correction at these stations may be attributed to a reduction in systematic errors and a better alignment between model outputs and observed values.

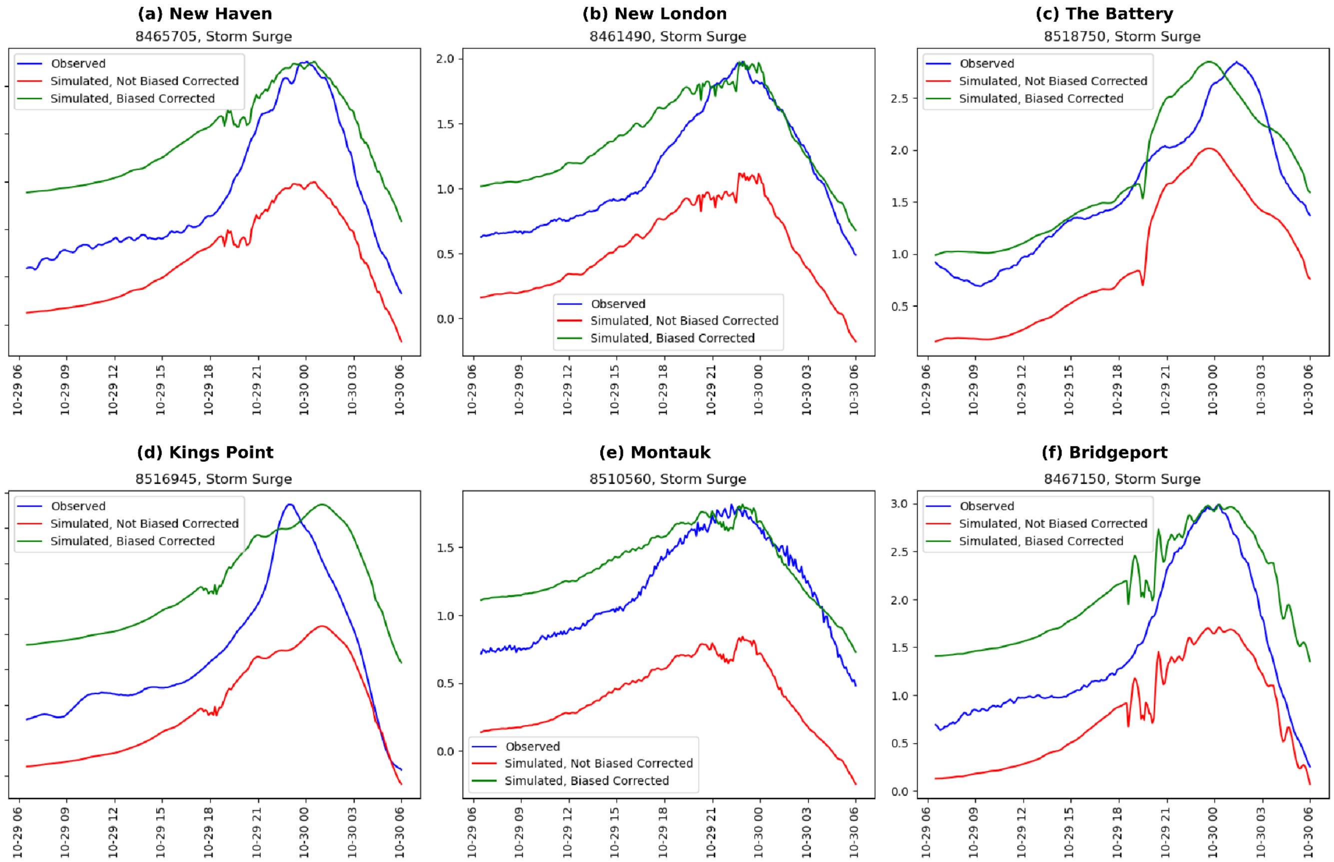

Figure S1: Comparison of observed, simulated, and maximum biased corrected simulated storm surges during Hurricane Sandy

Table S1: The evaluation metrics of simulated storm surges during Hurricane Sandy; a) without any bias correction; b) with maximum bias correction

a) Hurricane Sandy's Evaluation Metrics, No Bias Correction					
Station Name	Station ID	NSE	KGE	RMSE	R Squared
The Battery	8518750	0.189	0.569	0.711	-0.189
Kings Point	8516945	0.138	0.461	0.873	0.138
Montauk	8510560	-3.65	0.269	0.798	-3.655
Bridgeport	8467150	0.052	0.443	0.742	0.052
New Haven	8465705	-0.09	0.395	0.728	-0.09
New London	8461490	-1.09	0.403	0.635	-1.09

b) Hurricane Sandy's Evaluation Metrics, Biased Corrected					
Station Name	Station ID	NSE	KGE	RMSE	R Squared
The Battery	8518750	0.836	0.884	0.263	0.83
Kings Point	8516945	-0.228	0.366	1.04	-0.22
Montauk	8510560	0.487	0.65	0.264	0.4487
Bridgeport	8467150	0.225	0.488	0.671	0.22
New Haven	8465705	0.122	0.445	0.653	0.122
New London	8461490	0.481	0.654	0.315	0.48

The outcomes presented in the validation process of the GeoClaw provide a comprehensive representation of the model's ability to accurately simulate the maximum water level during hurricanes. Based on this demonstrated capability, we proceeded to conduct simulations for all the additional storms listed in Table 1. The storm surge results obtained from these simulations were utilized as input variables, while the corresponding flood depth values served as target variables for the machine learning algorithms employed in the analysis.

2. Hydrologic Modeling with NextGen CFE Model

We simulated river discharge for eight catchments in Manhattan, NYC, during nine storm events using the NextGen CFE hydrologic model.

Our analysis reveals noticeable differences in discharge rates across storm events and catchments. The discharge rates vary significantly across different storm events. The mean discharge rates, for instance, ranged from 4287.52 m^3/s to 91612.33 m^3/s. Hurricanes generally cause higher and more variable discharge rates than tropical storms. Specifically, Hurricane Irene (Figure S5) resulted in the highest mean discharge rates among all the storm events. This is consistent with our expectation that more severe weather events lead to greater volumes of rainfall and thus higher discharge rates.

Regarding the different catchments, the cat-694852 catchment consistently exhibited the highest discharge rates and the most variation across all storm events. In contrast, the cat-694722 catchment had the lowest rates and the least variation (Figure S2). This could be due to various factors such as the size and characteristics of the catchments, including their land use and soil type, and the capacity of their drainage systems.

While high discharge values are expected during storm events due to increased rainfall, the catchment area, the intensity of the storm, and the duration of the rainfall. For instance, urban areas with a high percentage of impervious surfaces (such as Manhattan) tend to have higher discharge rates compared to rural areas, as water cannot infiltrate into the ground and thus runs off into rivers and streams more quickly. However, these high values also underline the importance of adequate stormwater management strategies to mitigate flooding risks and protect urban environments during storm events.

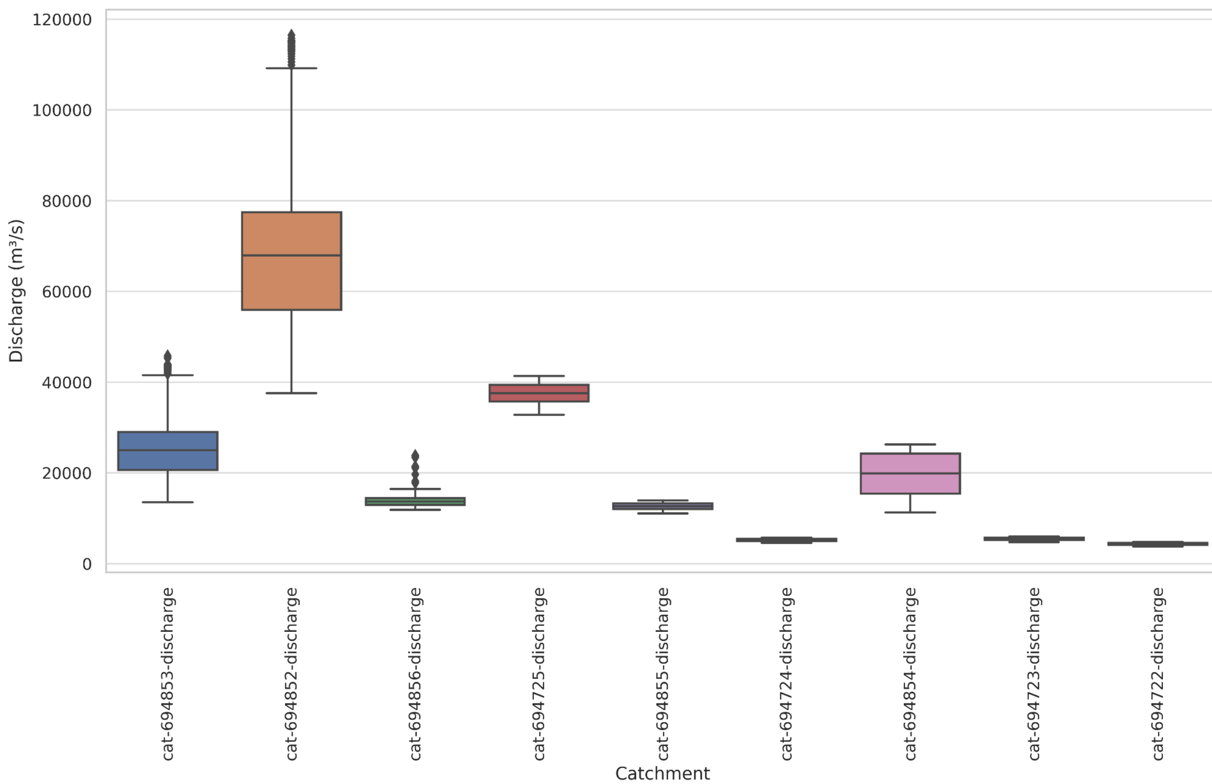

Figure S2: Boxplot showing the distributions of river discharge rates for different catchments during all nine storm events.

Below are the summary statistics (mean, median, standard deviation, minimum, maximum, and interquartile range) for the discharge rates (in m^3/s) of each catchment during each storm event:

- **Hurricane Arthur:** The mean discharge rates range from 4425.87 m^3/s (cat-694722) to 70971.85 m^3/s (cat-694852). The variation in discharge rates is also quite significant, with standard deviations ranging from 214.91 m^3/s to 11626.14 m^3/s.

- **Hurricane Dorian:** The mean discharge rates range from 4287.52 m^3/s (cat-694722) to 69092.53 m^3/s (cat-694852). The variation in discharge rates is slightly higher than during Hurricane Arthur, with standard deviations ranging from 288.22 m^3/s to 12041.82 m^3/s.

- **Hurricane Hanna:** The mean discharge rates range from 4497.85 m^3/s (cat-694722) to 64330.77 m^3/s (cat-694852). The variation in discharge rates is lower than during the previous two hurricanes, with standard deviations ranging from 175.96 m^3/s to 9879.14 m^3/s.

- **Hurricane Irene:** The mean discharge rates range from 4425.87 m^3/s (cat-694722) to 91612.33 m^3/s (cat-694852). This is the highest mean discharge rate observed in the dataset. The variation in discharge rates is also the highest, with standard deviations ranging from 214.91 m^3/s to 20169.28 m^3/s.

- **Hurricane Sandy:** The mean discharge rates range from 4355.79 m^3/s (cat-694722) to 77368.58 m^3/s (cat-694852). The variation in discharge rates is similar to that during Hurricane Arthur, with standard deviations ranging from 252.31 m^3/s to 14549.12 m^3/s.

- **Tropical Storm Barry:** The mean discharge rates range from 4355.79 m^3/s (cat-694722) to 62374.54 m^3/s (cat-694852). The variation in discharge rates is lower than during most of the hurricanes, with standard deviations ranging from 252.31 m^3/s to 8799.90 m^3/s.

- **Tropical Storm Jose:** The mean discharge rates range from 4355.79 m^3/s (cat-694722) to 61348.07 m^3/s (cat-694852). The variation in discharge rates is similar to that during Tropical Storm Barry, with standard deviations ranging from 252.31 m^3/s to 14803.46 m^3/s.

- **Tropical Storm Ogla:** The mean discharge rates range from 4355.79 m^3/s (cat-694722) to 56958.84 m^3/s (cat-694852). The variation in discharge rates is similar to that during the previous two tropical storms, with standard deviations ranging from 252.31 m^3/s to 11849.44 m^3/s.

- **Tropical Storm Philippe:** The mean discharge rates range from 4287.52 m^3/s (cat-694722) to 57497.49 m^3/s (cat-694852). The variation in discharge rates is similar to that during Hurricane Dorian, with standard deviations ranging from 288.22 m^3/s to 11197.53 m^3/s.

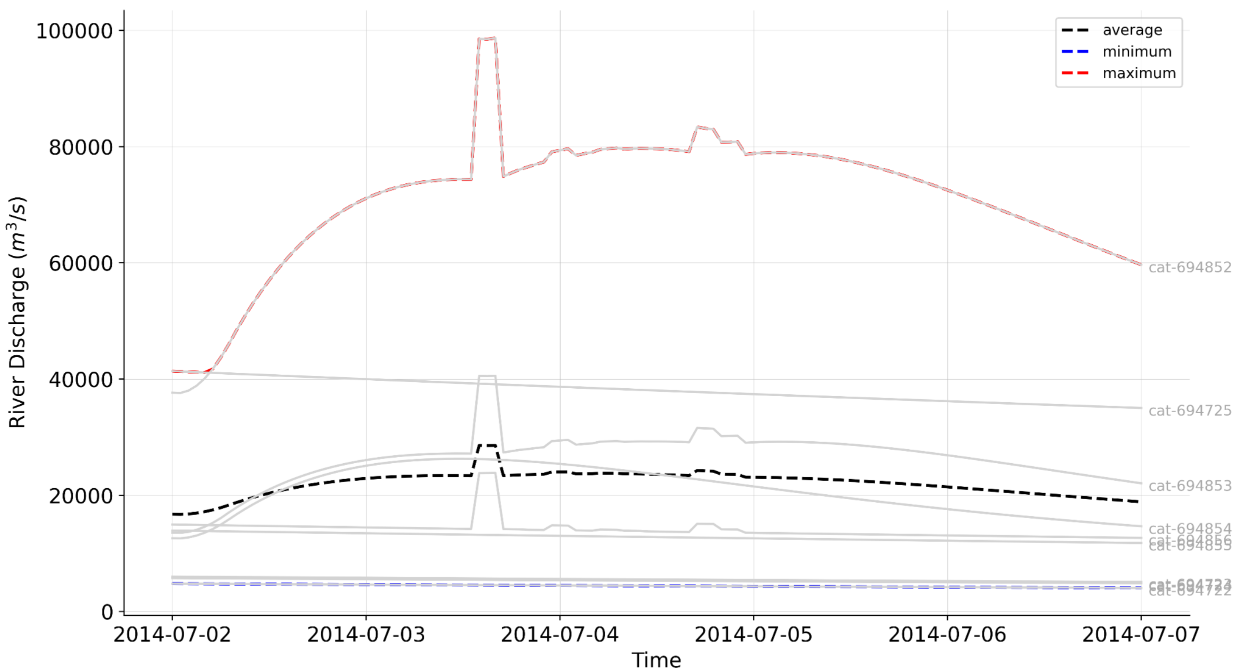

Figure S3: River discharge output from the NextGen CFE model during Hurricane Arthur (2014) for different catchments in the NYC area. The red color indicates the catchment with the highest discharge, the blue color indicates the catchment with the lowest discharge, and the black color indicates the average discharge during Hurricane Arthur.

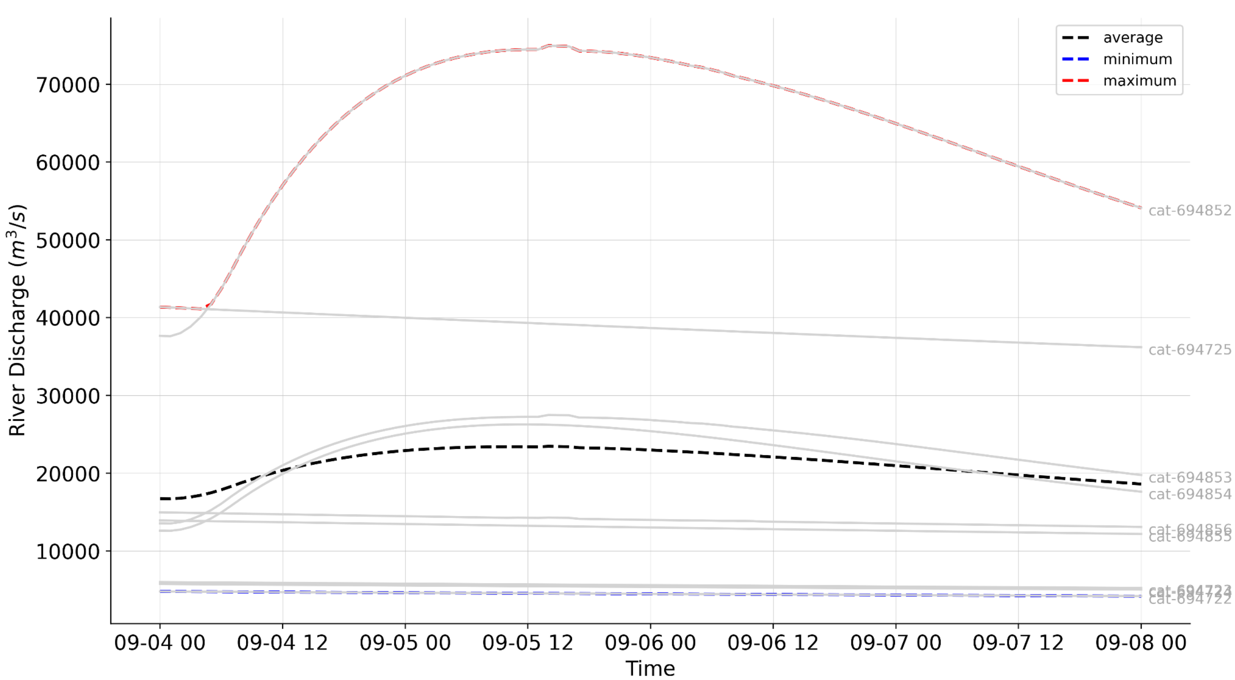

Figure S4: Same as Figure S2 but for Hurricane Hanna (2008).

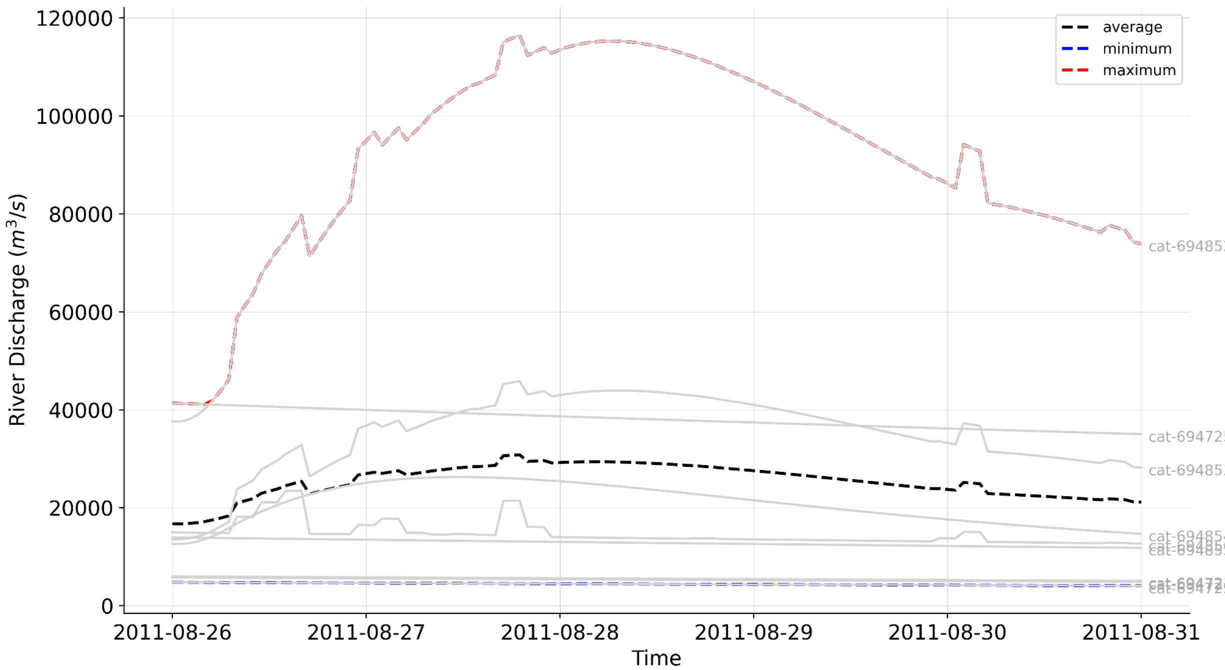

Figure S5: Same as Figure S2 but for Hurricane Irene (2011).

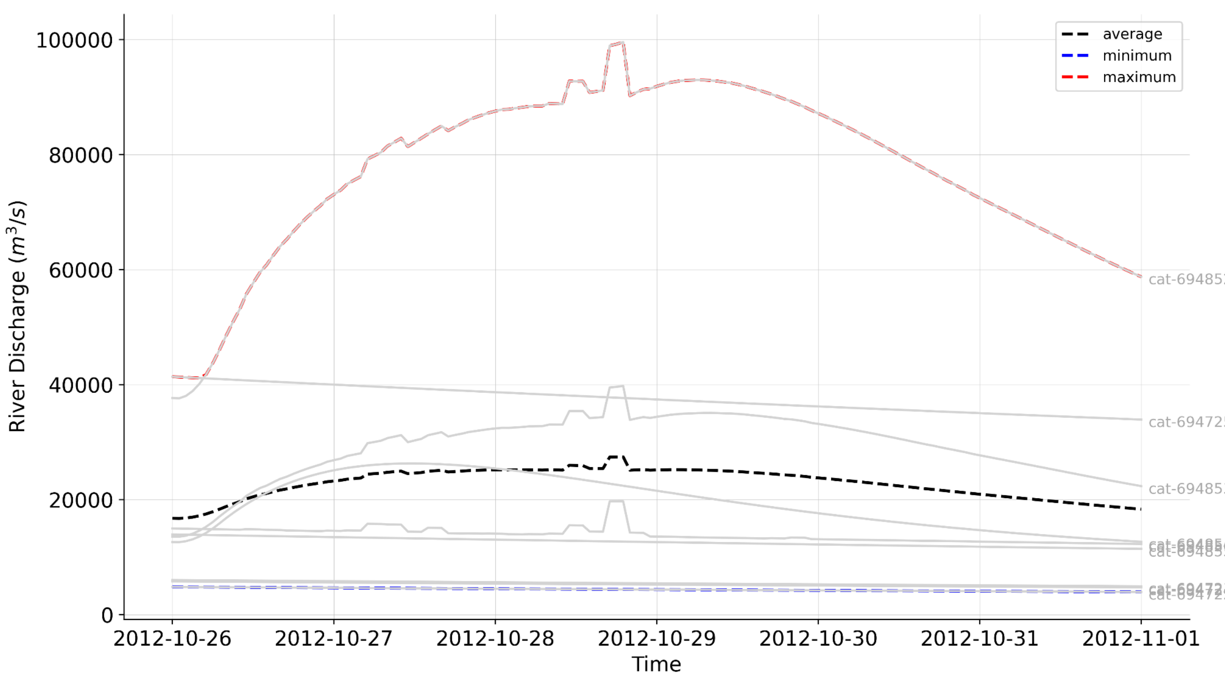

Figure S6: Same as Figure S2 but for Hurricane Sandy (2012).

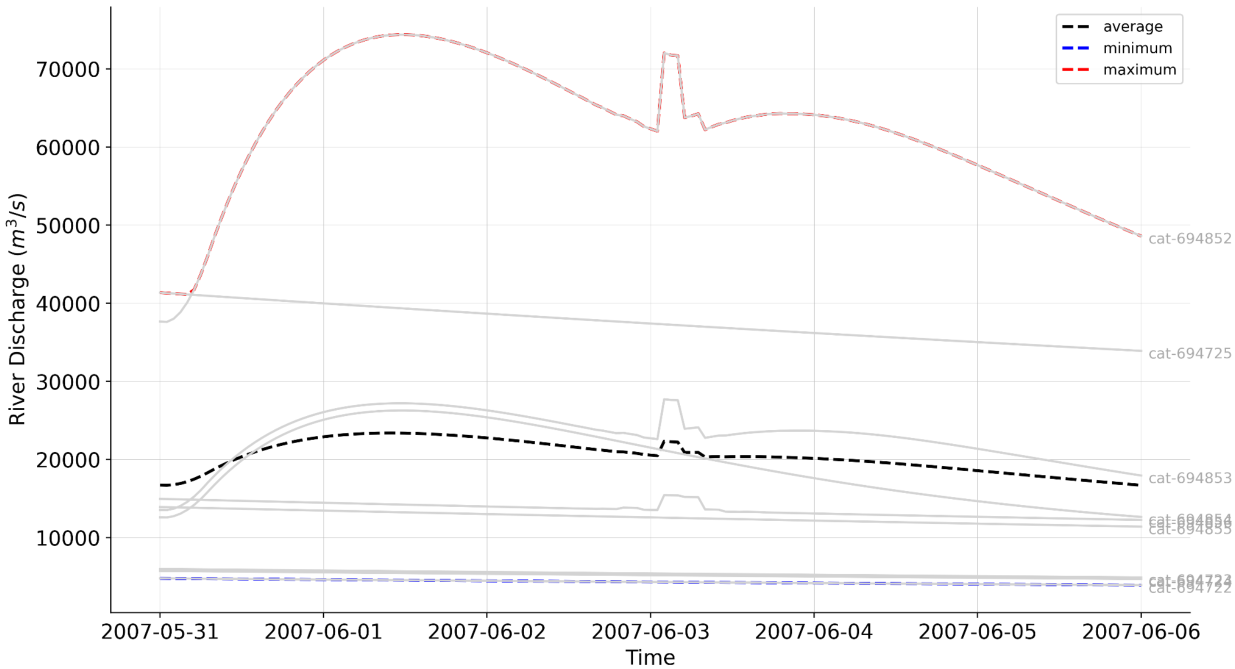

Figure S7: Same as Figure S2 but for Tropical Storm Barry (2007).

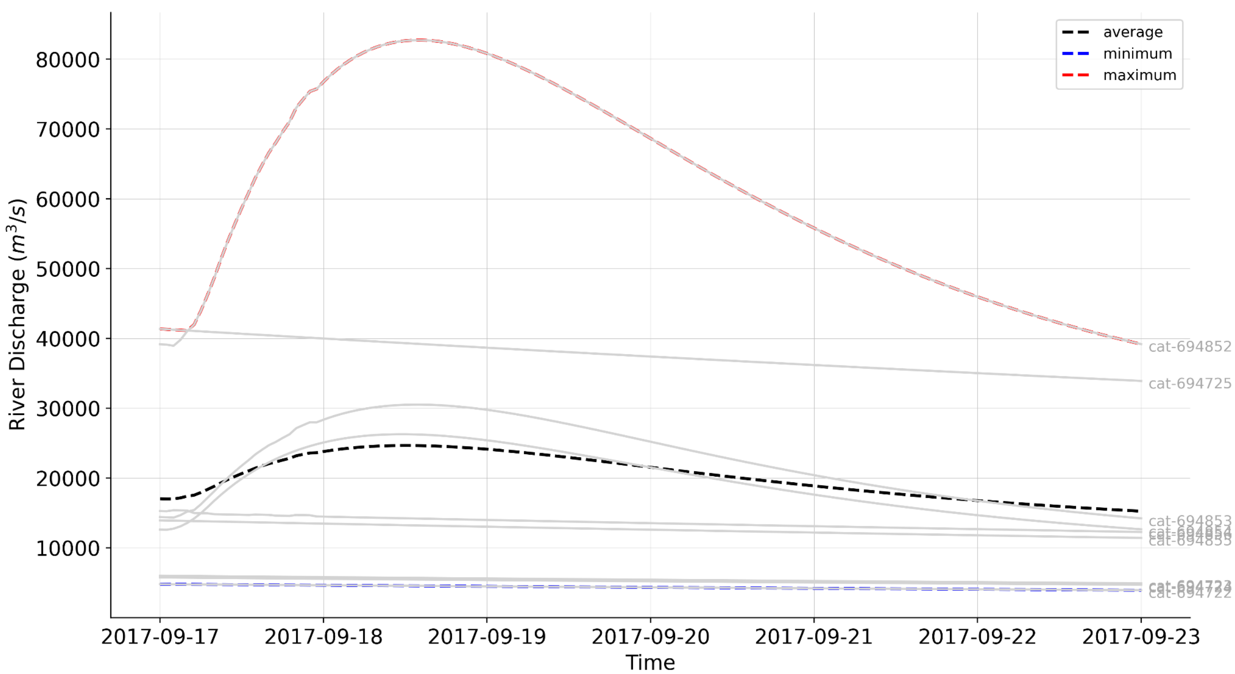

Figure S8: Same as Figure S2 but for Tropical Storm Jose (2017).

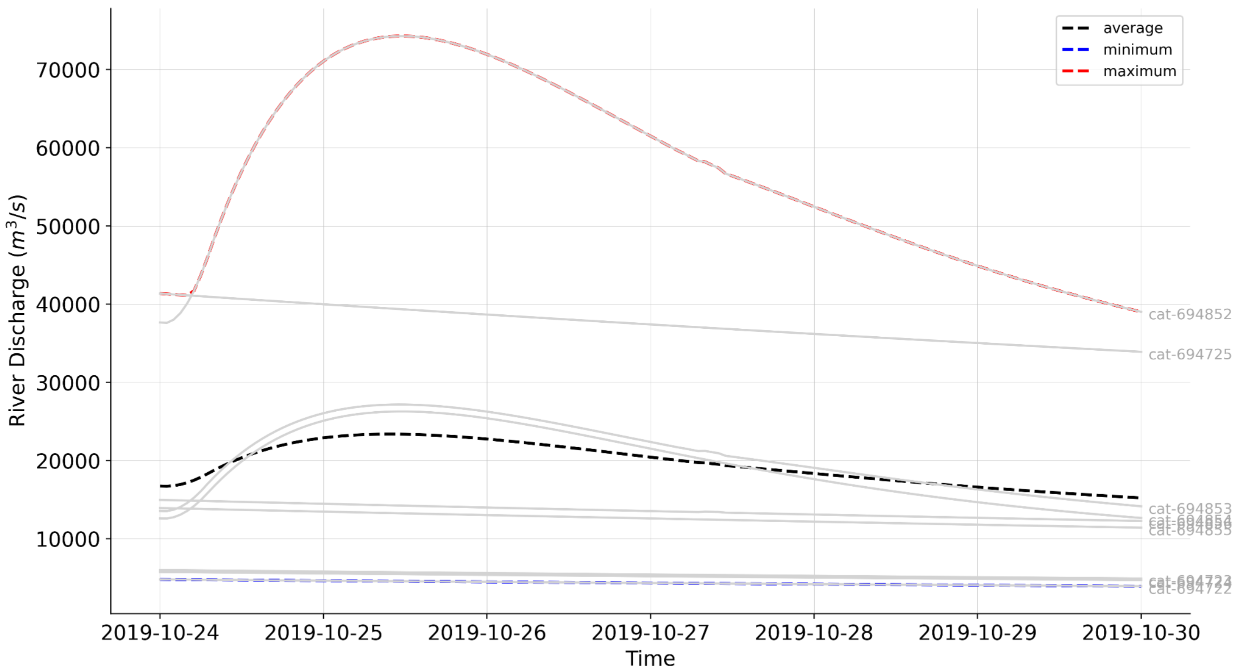

Figure S9: Same as Figure S2 but for Tropical Storm Ogla (2019).

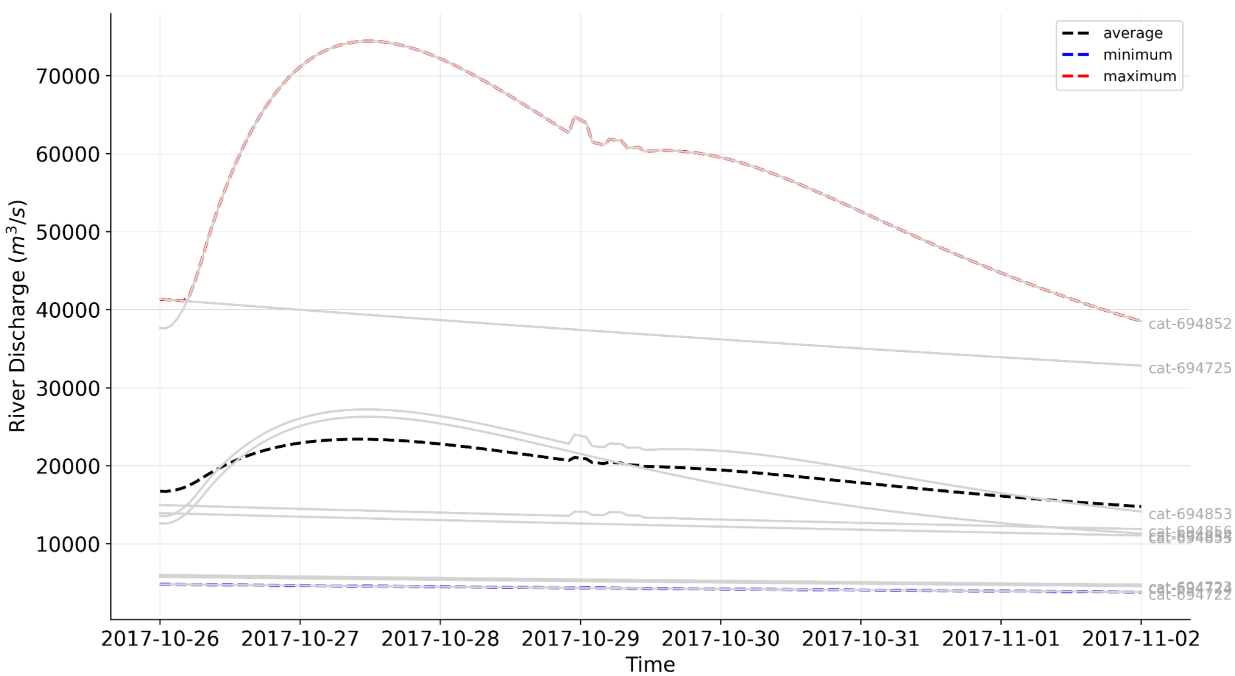

Figure S10: Same as Figure S2 but for Tropical Storm Philippe (2017).

3. Machine Learning

Figure S11 shows a pie chart that represents the relative importance of the three features (Precipitation, Storm surge, and River discharge) for different gauges in Manhattan, NYC. The size of each section of the pie corresponds to the importance of that feature at the gauge.

The results about the relative importance of different flood drivers in the Manhattan area provide the following insights.

- **Variability in Feature Importance:** The analysis shows significant variability in feature importance across different gauges. This suggests that flood prediction in different parts of Manhattan may require different emphasis on the three considered flood drivers.

- **The dominance of Precipitation:** In several gauges (like 8, 13, 18-22), precipitation (light blue) has the largest share in the pie charts. This implies that in these areas, rainfall is the most influential factor for flood prediction.

- **Surge Importance in Coastal Areas:** Surge (light red) becomes a dominant factor in several gauges (like 14-16, 20-29). Given that surge is associated with sea-level changes, it's plausible that these gauges are closer to the coast where tidal changes might significantly impact flood conditions.

- **Significance of Discharge in Certain Areas:** The discharge (light green) has a prominent role in some gauges (like 25-29). These areas might be near rivers or drains where the rate of water flow (discharge) is a critical factor for flood conditions.

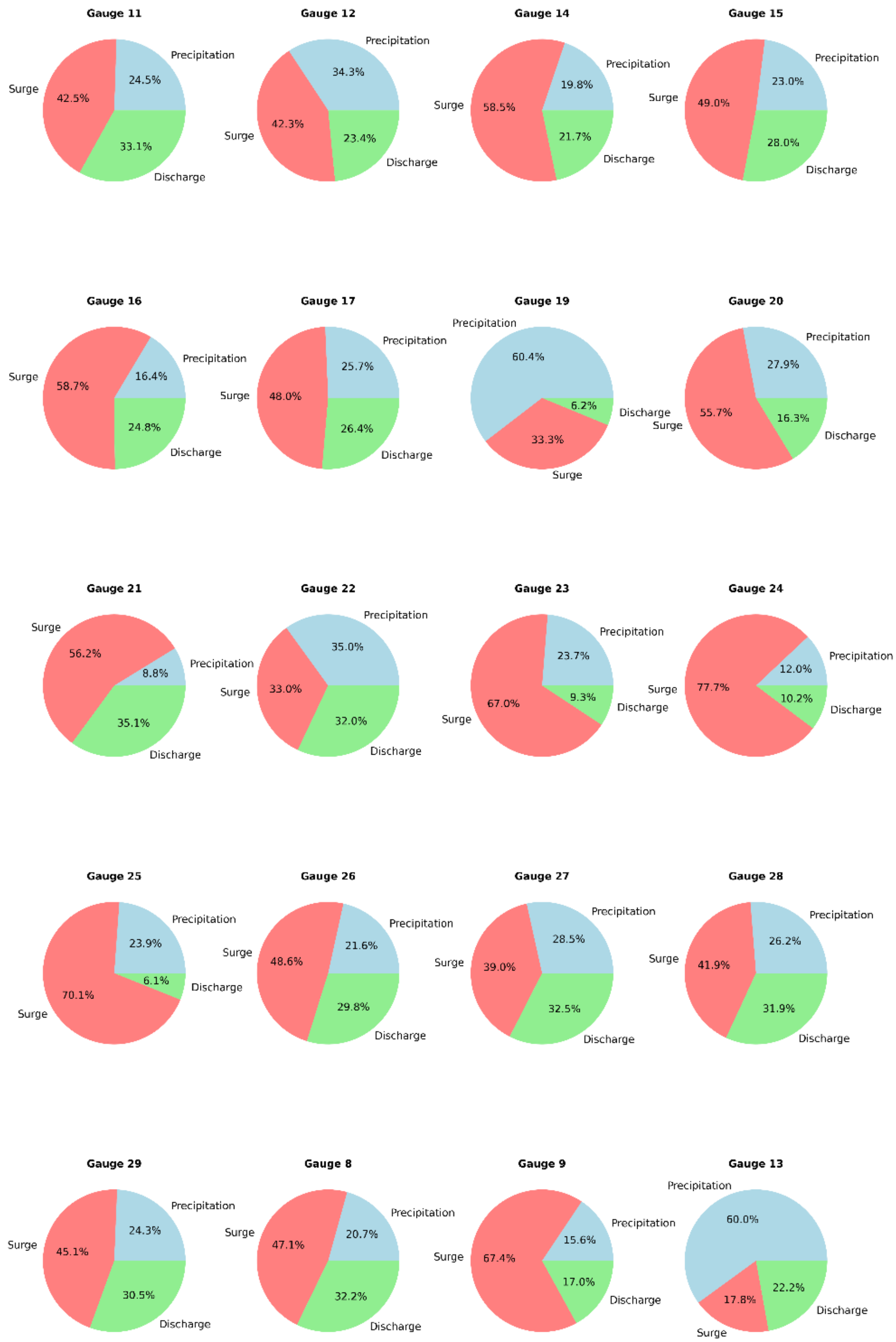

Figure S11: The pie chart representing the relative importance of the flood drivers (Precipitation, Surge, and Discharge) for specific gauges in Manhattan, NYC.